Self-association of Escherichia coli DNA-dependent RNA polymerase core enzyme

ARTICLE *in* BIOCHEMISTRY · AUGUST 1995

Impact Factor: 3.02 · DOI: 10.1021/bi00027a026 · Source: PubMed

3 AUTHORS, INCLUDING:

Simon J Harris
Monash University (Australia)
32 PUBLICATIONS **559** CITATIONS
SEE PROFILE

James Ching Lee
University of Texas Medical Branch at Galvest…
140 PUBLICATIONS **5,671** CITATIONS
SEE PROFILE

Self-Association of *Escherichia coli* DNA-Dependent RNA Polymerase Core Enzyme†

Simon J. Harris,‡,§ Robley C. Williams, Jr.,|| and J. Ching Lee*,§

Department of Human Biological Chemistry and Genetics, University of Texas Medical Branch, Galveston, Texas 77555-1055, and Department of Molecular Biology, Vanderbilt University, Nashville, Tennessee 37235

Received February 23, 1995; Revised Manuscript Received May 11, 1995⊗

ABSTRACT: The extent of self-association of *Escherichia coli* DNA-dependent RNA polymerase core enzyme has been investigated by velocity sedimentation as a function of both NaCl and protein concentrations. The core enzyme, existing as essentially monomeric species having a sedimentation coefficient of 13.1 S at NaCl concentrations greater than 0.2 M, undergoes reversible self-association at lower salt concentrations. Estimates for the stoichiometry of association and equilibrium constants of reaction were determined from the effect of protein concentration on the weight-average sedimentation coefficient measured at different NaCl concentrations. Data analysis by a nonlinear curve-fitting procedure indicated that protein self-association is best described by a sequential model characterized by weaker association constants for each additional step of oligomerization, and any model that involves cooperative formation of oligomeric species can be excluded. These findings are at variance with the conclusion of a previous study [Shaner, S. L., Platt, D. M., Wensley, C. G., Yu, H., Burgess, R. R., & Record, M. T. (1982) *Biochemistry 26,* 5539−5551] which suggested that core RNA polymerase exists in equilibrium between monomeric and tetrameric forms of the enzyme and excluded the existence of intermediate species. Simulation of sedimentation velocity boundary and gradient profiles are used to assess the validity of both models of association of core protein. It was clear that had the core enzyme undergone a cooperative monomer ⇌ tetramer mode of association, then bimodality would have been observed in the derivative tracings of the sedimentation boundary under these experimental conditions. Nevertheless, no such observation was reported by Shaner et al. and this study. The sequential model favored by the results of this study is consistent with the proposed model resulted from a small-angle X-ray study [Heumann, H., Meisenberger O., & Pilz, I. (1982) *FEBS Lett. 138,* 273−276]. Further analysis of the data by the Wyman linked-function relationship [Wyman, J. (1964) *Adv. Protein Chem. 19,* 223−286] implies that core enzyme monomer loses approximately three counterions per contact upon association to higher oligomeric species.

The DNA-dependent RNA polymerase of *Escherichia coli* (EC 2.7.7.6) is a multisubunit protein that occurs in two forms, comprising four different polypeptide chains in the holoenzyme ($\alpha_2\beta\beta'\sigma$: M_r = 45 0000) which reversibly dissociates into the core enzyme ($\alpha_2\beta\beta'$: M_r = 380 000) and the σ factor (Burgess, 1969b; Berg et al., 1971). The holoenzyme binds DNA and initiates specific transcription in the absence or presence of other DNA-binding regulatory proteins including cyclic-AMP receptor protein (CRP); interaction between RNA polymerase and CRP *in vitro* has been reported to be both dependent and independent of the presence of DNA (Nissley et al., 1972; Wu et al., 1974; Blazy et al., 1980; Malan et al., 1984; Spassky et al., 1984; Pinkney & Hoggett, 1988; Heyduk et al., 1993). Once chain elongation has begun, the σ factor dissociates from the holo RNA polymerase as the core RNA polymerase continues to move along the DNA molecule and synthesizes RNA. The dissociated σ factor can subsequently bind to another core RNA polymerase, which is incapable of binding to promoter DNA and effectively initiating transcription, thereby allowing a new round of transcription to occur (Burgess et al., 1969; Travers & Burgess, 1969; Burgess, 1971; Wu et al., 1975; Chamberlin, 1976).

It has been reasonably well documented that both holo and core RNA polymerase exist in different states of aggregation as a function of salt concentration (Richardson, 1966; Stevens et al., 1966; Burgess, 1969a; Berg & Chamberlin, 1970; Shaner et al., 1982; Heumann et al., 1982). These results have led to the proposal that the extent of aggregation of RNA polymerase provides a mechanism for regulation of transcription from different promoters (Travers et al., 1982). However, there is limited amount of information that adequately describes the modes of protein self-association, equilibrium constants between various oligomeric species in solution, or the potential role played by this phenomenon in the regulation of transcription. An effort has been made to characterize the self-association of both *E. coli* RNA polymerase holo and core proteins. Sedimentation velocity ultracentrifugation data indicated different modes of association for both forms of the enzyme (Shaner et al., 1982). In the absence of Mg^{2+} ion these authors suggested that holoenzyme undergoes anion-dependent dimerization, whereas core protein self-associates cooperatively to tetramer; the presence of Mg^{2+} caused aggregation of core

† Supported by NIH Grants GM-25638 (to R.C.W.) and GM-45579 and by Robert A. Welch Foundation Grants H-0013 and H-1238 (to J.C.L.).

* Author to whom correspondence should be addressed.

‡ Present address: Department of Biochemistry, Baker Medical Research Institute, Victoria 3181 Australia.

§ University of Texas Medical Branch.

|| Vanderbilt University.

⊗ Abstract published in *Advance ACS Abstracts,* June 15, 1995.

0006-2960/95/0434-8752$09.00/0

enzyme to octamer without having further effect upon the aggregation state of holoenzyme. Since the stoichiometry of the RNA polymerase association reaction is greater than 2 as reported by Shaner et al., a cooperativity of aggregation is suggested. Furthermore, a proposed stoichiometry of 4 for the self-association of RNA polymerase core protein should lead to bimodality in the derivative curves of the sedimentation velocity boundaries as predicted by theory (Gilbert, 1955, 1959, 1963), but not reported as an experimental observation. The validity of the proposed two-state model is therefore open to question and deserving of further scrutiny.

In order to provide a thermodynamic characterization of this aggregation phenomenon, an extensive sedimentation velocity ultracentrifugation study of the self-association of purified *E. coli* RNA polymerase core protein was conducted as a function of both salt and protein concentrations. Our data analysis presents a sequential self-association model of this enzyme. Models involving cooperative formation of oligomeric species can be excluded. Comparison of experimental and computer simulated sedimentation velocity boundary and gradient profiles has been used to assess the validity of the variant models for protein self-association. Light scattering is used to confirm the basic tenets of the step-wise association model that emanates from the sedimentation studies.

MATERIALS AND METHODS

All experiments with *E. coli* polymerase core protein were conducted at 20 °C in buffer comprising 50 mM Tris (pH 7.8), 1 mM EDTA, and 1 mM DTT (TED buffer) supplemented with appropriate concentration of NaCl. Spectrophotometric determination of protein concentrations were obtained using an absorption coefficient ($E^{1\%}_{1cm}$) of 5.50 at 280 nm (Burgess, 1976) and molecular weight of 380 000 (Berg & Chamberlin, 1970; Pilz et al., 1972) for core RNA polymerase.

Purification of Core RNA Polymerase. A mixture of both RNA polymerase holo and core proteins was purified from 500 g of *E. coli* K12 cells according to a modification (Lowe et al., 1979) of the method of Burgess and Jendrisak (1975); purified RNA polymerase core protein was subsequently obtained by removal of σ factor from the holoenzyme by chromatography through a Bio-Rex 70 column and subsequently stored at −20 °C in storage buffer containing 10 mM Tris (pH 7.9), 0.1 mM EDTA, 0.1 mM DTT, and 50% glycerol until required. Enzymic activity of RNA polymerase was determined by the assay of Chamberlin et al. (1979) using calf thymus DNA as template. Protein solution was better than 95% pure as judged by SDS−polyacrylamide gel electrophoresis.

Sample Preparation. Protein samples used in investigations were dialyzed against TED buffer supplemented with appropriate NaCl to remove glycerol, clarified by centrifugation for 30 s in a Beckman benchtop microfuge, and then diluted to the required concentration with the same buffer.

Sedimentation Velocity. Sedimentation velocity experiments were performed at 20 °C using a Beckman Model E analytical ultracentrifuge equipped with an electronic speed control, monochrometer, ultraviolet photoelectric scanner with multiplexer, and RTIC temperature control unit. Double-sector, charcoal-filled Epon centerpieces and sapphire windows were used in AN-E rotors at 52 000 rpm. Digital scans of reaction boundaries were obtained at 280 nm and recorded on an IBM PS/2 computer linked to the scanner and multiplexer unit. Weight-average sedimentation coefficients ($\bar{S}_{20,w}$) at all defined total protein concentrations were determined from an approximation of the second moment of digitized scanner traces of the reaction boundary (Arisaka & Van Holde, 1979) and normalized to standard conditions after correction for solvent density and viscosity.

For any model-independent system undergoing self-association the weight-average sedimentation coefficient can be determined from

$$\bar{s} = \sum s_i C_i / \sum C_i \quad (1)$$

where s_i and C_i are the sedimentation coefficients and equilibrium concentrations of the ith species, respectively (Schachman, 1959). Therefore, weight-average sedimentation coefficient can be expressed as a function of protein monomer (C_1) concentration as

$$\bar{s} = \sum s_i^\circ (1 - g_i C_{tot}) K_i C_1^i / \sum K_i C_1^i \quad (2)$$

where s_i° is the sedimentation coefficient of the ith species extrapolated to infinite dilution, g_i is the respective hydrodynamic nonideality coefficient, $C_{tot} = \Sigma K_i C_1^i$ and K_i is the Adair equilibrium intrinsic association constant between monomer and any i-meric species present in solution. K_1 is equal to unity, by definition.

The data obtained from these experiments were analyzed using a nonlinear least-squares curve-fitting procedure (Marquardt, 1963) previously adopted in this laboratory (Hesterberg & Lee, 1981, 1982; Luther et al., 1986; Callaci et al., 1990). Thus, estimates of the interaction parameters that best describe self-association for RNA polymerase core protein have been determined from the best-fit of the protein concentration-dependence of $\bar{s}$ at fixed salt concentration.

In the curve-fitting procedure attempts were made to fit the weight-average sedimentation coefficient to every reasonable model for core protein self-association in order to determine the model that best describes aggregation phenomenon. The various models include a variety of two-state models, sequential polymerization and isodesmic association.

Criteria for Model Selection. In analyzing the data to determine the stoichiometry and equilibrium constant, it became evident that, under certain conditions, more than one mode can describe the data equally well. Hence, the following set of rules was adopted to aid in assessing the reliability of data analysis.

(1) Use either the standard root mean square deviation (σ) or sum of squares of residuals (SS) to select the mode of association. The lower the value of σ or SS, the better are the calculated data compared with those determined experimentally.

(2) If two or more modes of association have equal or very similar σ values, then the mode with the smallest number of species is chosen.

(3) If rules 1 and 2 cannot allow differentiation between modes of association, then only those equilibria with consistent values for apparent association constants K_i^{app} are included in the final data analysis.

Assumption of Molecular Geometry. In these data analyses, an estimate of the $S^\circ_{20,w}$ for the species undergoing

Table 1: Frictional and Sedimentation Coefficients for Oligomers of *E. coli* RNA Polymerase Core Protein[a]

i	S_i° [b]	$(f/f_o)^c$	S_i° [c]	$(f/f_o)^d$	S_i° [d]
1	13.10	1.000	13.10	1.000	13.10
2	20.80	1.042	19.96	1.044	19.92
3	27.25	1.105	24.66	1.112	24.50
4	33.01	1.165	28.33	1.182	27.93
5	38.30	1.224	31.29	1.255	30.42
6	43.26	1.277	33.87	1.314	32.92
8	52.40	1.374	38.14	1.433	36.57

[a] Values were calculated using the spherical geometry approximation [eq 3 and Schachman (1959)] where value for monomer species of 13.10 S determined from linear regression through concentration dependence of weight-average sedimentation coefficient in TED buffer containing 0.25 M NaCl. Frictional coefficients have been taken from Table IX of Schachman (1959) and correspond to oligomers having proportionate axial ratios when considered as ellipsoids of revolution. [b] Sedimentation coefficients for oligomers exhibiting identical behavior characteristic of globular proteins, i.e., $f/f_o = 1.000$. [c] Frictional and calculated sedimentation coefficients for oligomers considered as oblate ellipsoids of revolution. [d] Frictional and calculated sedimentation coefficients for oligomers considered as prolate ellipsoids of revolution.

association is required. In the absence of definitive values of sedimentation coefficients for different oligomeric species of RNA polymerase core protein other than monomer (13.1 S), estimates for values of ith species can be obtained by assuming spherical geometry relationship (Schachman, 1959)

$$s_i^{\circ} = s_1^{\circ}(M_i/M_1)^{2/3}/(f/f_o) \quad (3)$$

where M_i and M_1 are the molecular weights of the associating species with i and 1 subunits, respectively; f is the frictional coefficient of the associating species and f_o is the frictional coefficient of a spherical molecule with the same mass and partial specific volume. It is reasonable to make the initial assumption here that all oligomeric species exhibit behavior typical of globular proteins having identical frictional ratios, i.e., $f/f_o = 1$ (Cann, 1970; Nichol et al., 1964).

In order to investigate the effect of the assumption of spherical geometry relationship in the uniqueness of the mode of RNA polymerase self-association, curve-fitting analysis of experimental data were also conducted by considering the higher oligomeric species of RNA polymerase core protein as being either oblate or prolate ellipsoids of revolution. Values of standard sedimentation coefficients used in this analysis are summarized in Table 1.

Light Scattering. Protein solutions were exhaustively dialyzed against TED buffer with 50 mM NaCl to remove glycerol, clarified by centrifugation,and then filtered through a membrane filter to remove insoluble particles after being adjusted to the required concentration. Scattering measurements were carried out at 633 nm wavelength and 20 °C in a Chromatix KMX-6 small-angle photometer as described by Williams (1986), with the use of angular ranges 2−3°, 4−5°, and 6−7°. Solutions were introduced into the photometer's flow-cell through membrane filters (Millipore filter Type HA, 0.45 μm, followed by Type GS, 0.22 μm) that remained in the flow circuit for the duration of the experiment.

RESULTS

Reversibility of Aggregation Equilibrium. Before any attempt can be made to quantify self-association phenomena, it is important to ascertain that the observed changes in sedimentation coefficient reflect existing rapid equilibria. The criterion is the independence of $\bar{S}_{20,w}$ as a function of rotor speed. The effects of rotor speed were investigated at fixed protein and salt concentration at rotor speeds varying between 15 000 and 52 000 rpm. Protein solutions were first sedimented at either high or low speed, mixed, and then sedimented again at incremental lower or higher rotor speeds, respectively. The effects on measured values of $S_{20,w}$ were negligible at all rotor speeds tested in this manner. These results established that the self-association is rapid and reversible. The data are, therefore, amenable to further analysis for equilibrium constants and stoichiometry.

The effect of NaCl concentration on the reversibility of self-association of core RNA polymerase is further tested by monitoring the ability to recover the same value of $\bar{S}_{20,w}$ after subjecting the system to a perturbation by a change in salt concentration. Solutions of *E. coli* RNA polymerase (0.72 mg/mL) were initially subjected to sedimentation velocity at low salt concentration (TED buffer containing 0.01 M NaCl); samples recovered and dialyzed against TED buffer containing NaCl at a concentration greater than 0.20 M; protein concentration adjusted to 0.72 mg/mL and again subjected to sedimentation velocity. This procedure was then adopted in reverse to return to low salt concentration. An alternative approach was to subject a protein solution, previously dialyzed against low or high salt buffer, to removal of buffer by ultrafiltration through Amicon YM-10 membranes, followed by three washes with a buffer containing the appropriate NaCl concentration; this concentrated protein was then collected in the same buffer, diluted to the desired protein concentration, and subjected to sedimention. This procedure was then repeated to change salt concentration of protein solution. A perturbation of the aggregation state of the enzyme by either of the above mentioned protocols yields essentially identical results. These results clearly attest to the reversibility of the self-association equilibrium for this protein under all the salt concentrations tested in this study.

Salt Concentration Dependence of Self-Association. Having demonstrated that the self-association behavior of RNA polymerase is a true thermodynamic phenomenon, the salt concentration dependence of weight-average sedimentation coefficient of core RNA polymerase was obtained at the same fixed core protein concentration (0.72 mg/mL) by varying the salt concentration over the range of 0.01−0.25 M in either NaCl or KCl. The data, presented in Figure 1, exhibit behavior that is qualitatively similar to that previously reported for this protein (Shaner et al., 1982) but have significant quantitative differences. The effects of both NaCl and KCl on the aggregation of core RNA polymerase are apparently identical, a fact which supports the conclusion that the observed effect could arise from specific interaction of anion with negatively charged core protein (Shaner et al., 1982). At salt concentrations greater than 0.20 M, core protein appears to sediment as a homogeneous species having an apparent $\bar{S}_{20,w}$ of 13.1 S. The weight-average sedimentation coefficient increases to 22.4 S at salt concentrations below 0.05 M. The value of sedimentation coefficient in the plateau region is lower than that of 26.7 S reported previously in the absence of Mg^{2+} (Shaner et al., 1982). In both instances, the plateau region reflects the weight distribution of the various oligomeric species at equilibrium. Hence,

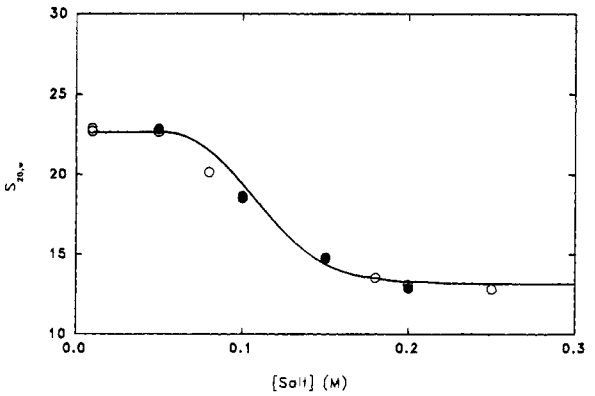

FIGURE 1: Salt concentration dependence of weight-average sedimentation coefficient for *E. coli* RNA polymerase core protein. Results were obtained from velocity sedimentation of fixed total core protein concentration (0.72 mg/mL) following extensive dialysis against TED buffer comprising 50 mM Tris (pH 7.8), 1 mM EDTA, and 1 mM DTT supplemented with either NaCl (○) or KCl (●). All experiments were performed at 52 000 rpm and 20 °C in Beckman Model E analytical ultracentrifuge. Weight-average sedimentation coefficients have been corrected to standard conditions. The curve drawn through data points is theoretical dependence of weight-average sedimentation coefficient deduced from eqs 2 and 4 for RNA polymerase core protein exhibiting sequential self-association of monomers. Appropriate values for K_i have been determined from linear regression through Wyman plots for salt concentration dependence of respective K_i values describing self-association (Figure 8).

the specific value of $\bar{S}_{20,w}$ depends on mode of association, association constant(s), and protein concentration. The observed difference in the value of $\bar{S}_{20,w}$ between the two studies does not necessarily reflect a difference in the intrinsic mode of association of the enzyme. A more complete study is required to elucidate the mechanism of self-association of the core enzyme.

Protein Concentration Dependence of Self-Association. The effect of protein concentration (0.05−4.00 mg/mL) on the weight-average sedimentation coefficient was determined under conditions of a fixed NaCl concentration. The data presented in Figure 2 clearly show differences in the extent of core protein self-association as NaCl concentration is increased from 0.01 to 0.25 M. The result obtained in buffer containing 0.01 M NaCl provides a typical example for a polymerizing system. The weight-average sedimentation coefficient initially increases with increasing protein concentration, indicating a system undergoing association−dissociation, then approaches a plateau and subsequently decreases in a linear fashion, as a consequence of hydrodynamic nonideality (Schachman, 1959), as protein concentration is further increased. Extrapolation through this linear region of the curve yields an estimate of 0.12 mL/mg for g, the solution hydrodynamic nonideality coefficient of eq 2. This value represents a balance between the opposing factors of protein self-association and solution nonideality. The larger-than-normal magnitude of this coefficient may be attributed to the extreme nonideality encountered in a buffer containing such low concentration of salt as a result of the primary-charge effect. Consequently, the apparent sedimentation coefficient is depressed due to differential sedimentation of charged macromolecule and its counterions.

In nearly all NaCl concentrations used in these investigations the value of $\bar{S}_{20,w}$ increases with increasing protein concentration. These results imply that RNA polymerase

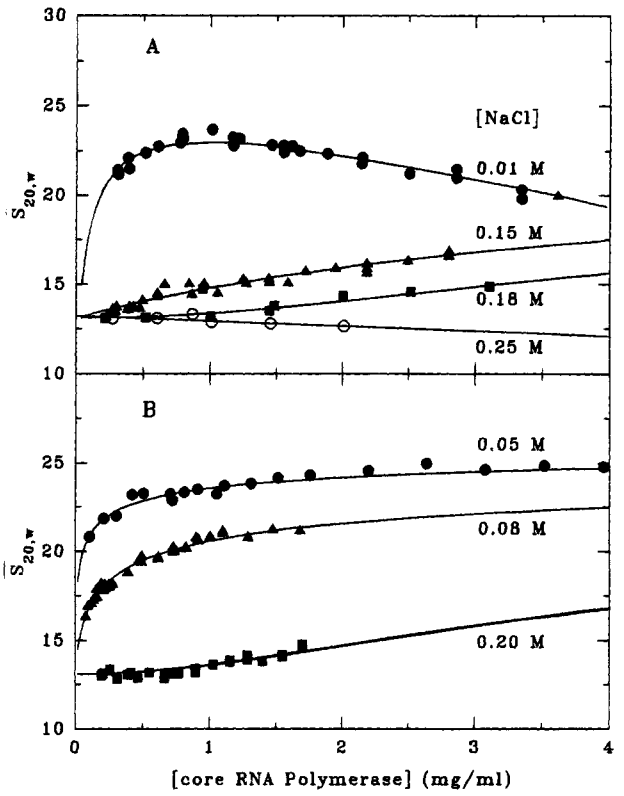

FIGURE 2: Protein concentration dependence of *E. coli* RNA polymerase core protein self-association phenomenon. Weight-average sedimentation coefficients, corrected to standard conditions, were determined from velocity sedimentation experiments performed at 52 000 rpm and 20 °C in TED buffer supplemented with NaCl concentrations indicated. Curves drawn through data points are theoretical fitted curves for core protein undergoing sequential self-association scheme terminating at trimer determined from nonlinear regression computer curve-fitting routine (see text for details). Line drawn through experimental data points obtained in buffer containing 0.25 M NaCl is linear least-squares regression line extrapolated to infinite protein dilution.

aggregates under these experimental conditions. The large solution nonideality effect observed in 0.01 M NaCl buffer apparently disappears at higher NaCl concentrations. Clearly, RNA polymerase core protein does not exist as purely monomer in 0.20 M NaCl buffer as evidenced by the apparently linear increase in weight-average sedimentation coefficient at protein concentrations greater than 1 mg/mL. However, at 0.25 M NaCl the weight-average sedimentation coefficient decreases in a linear fashion as protein concentration increases, according to the classical equation $S_{20,w} = S^{o}_{20,w}(1 - gC_{tot})$. Linear least-squares analysis through this data set yields a value of 0.045 mL/mg for the hydrodynamic nonideality coefficient, a value approximately one order of magnitude higher than that expected for a nonassociating globular protein (Teller, 1973). The ordinate intercept yields a sedimentation coefficient extrapolated to infinite dilution, $S^{o}_{20,w}$, of 13.2 ± 0.08 S. In combination of the results shown in Figure 1 the sedimentation coefficient of 13.1 S is adopted for monomeric core RNA polymerase.

In a system undergoing cooperative self-association equilibrium between monomer and oligomers larger than dimer, bimodal derivatives of the sedimentation boundaries should become evident with increasing protein concentration (Gilbert, 1955, 1959, 1963). Examination of moving-boundary profiles obtained in these experiments showed no evidence of bimodality for any protein concentration at fixed NaCl

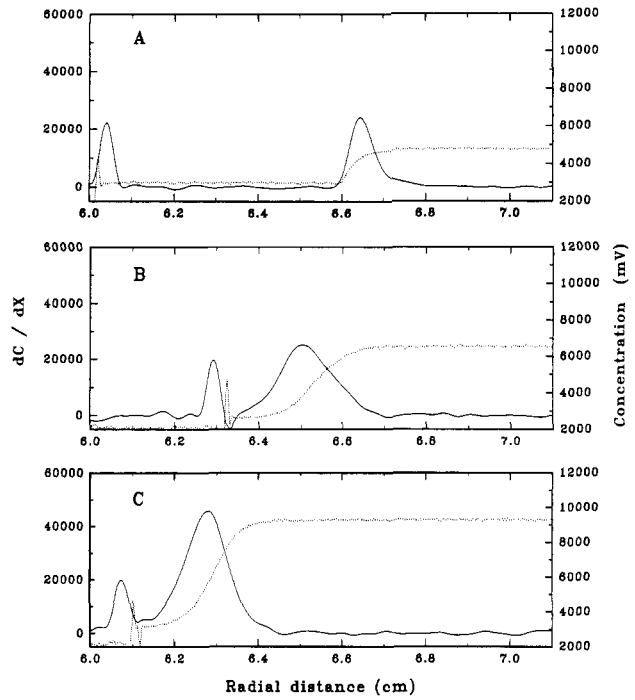

FIGURE 3: Experimental sedimentation velocity profiles of RNA polymerase core protein in TED buffer with 0.01 M NaCl at pH 7.8 and 20 °C. The experimental conditions are as follows: (A) 0.29 mg/mL, 30 000 rpm, 68 min; (B) 1.0 mg/mL, 24 000 rpm, 35 min; (C) 1.75 mg/mL, 24 000 rpm, 35 min. In each frame, the derivative curve is superimposed on the reaction boundary.

concentration. Typical profiles at three different protein concentrations are shown in Figure 3. This suggests that RNA polymerase core protein undergoes a sequential mode of self-association and not the two-sate model previously suggested for this protein system (Shaner et al., 1982).

Determination of Parameters Describing Self-Association of Core Protein. Parameters for the extent of core protein self-association, including stoichiometry of association and intrinsic association constants for the equilibria between oligomeric species, have been obtained from nonlinear analysis of the protein concentration dependence of weight-average sedimentation coefficient. Theoretical estimates for these parameters can be obtained from eq 2 as a function of C_1, s_i^o, g_i, and K_i fitted to the observed dependence of weight-average sedimentation coefficient upon total core protein concentration. Using the calculated values of s_i^o for different oligomeric species and preliminary estimates for g_i and K_i, refined values of these parameters were obtained by a reiteration scheme to ensure minimization of the sum of the residual squared (SS) convergence criterion for each set of concentration-dependence data at fixed NaCl concentration. Hence, the scheme that globally best describes self-association of RNA polymerase core protein can be determined from that which yields the lowest SS value at all NaCl concentration. Results from this approach are summarized in Tables 2 and 3, where s_i^o values used are those calculated for oligomers with the assumption of the spherical and other geometry approximation, respectively. Values for equilibrium intrinsic association constant are Adair constants for association of monomer to the indicated oligomer; units are expressed in terms of $(mL/mg)^{i-1}$. Not all of the possible models are presented in Tables 2 and 3 as it was impossible to obtain adequate fittings for certain modes of protein aggregation, e.g., two-state systems having stoichiometry of

Table 2: Summary of Fitted Equilibrium Intrinsic Association Constants for Self-Association of *E. coli* RNA Polymerase Core Protein as a Function of NaCl Concentration[a]

[NaCl] (M)	schemes	K_2 (mL/mg)	K_3 $(mL/mg)^2$	K_4 $(mL/mg)^3$	g	SS
0.01	1−3		498		0.13	8.42
	1−2−3	**0.19**	**494**		**0.13**	**8.44**
	1−2−3−4	0.21	526	42	0.13	9.06
0.05	1−3		129		0	69.2
	1−2−3	**169**	**3500**		**0**	**4.75**
	1−2−3−4	192	4020	780	0	3.24
0.08	1−3		17.1		0	254
	1−2−3	**12.9**	**23.5**		**0**	**4.75**
	1−2−3−4	13.2	21.3	7.44	0	4.49
0.15	1−3		0.45		0	46.5
	1−2−3	**0.55**	**0.21**		**0**	**11.9**
	1−2−3−4	0.57	0.20	2.51×10^{-3}	0	12.1
0.18	1−3		0.08		0	0.70
	1−2−3	**0.01**	**0.08**		**0**	**0.70**
	1−2−3−4	0.01	0.08	6.00×10^{-5}	0	0.71

[a] Values for thermodynamic parameters governing self-association have been obtained using eq 2 where sedimentation coefficients of oligomers have been calculated on basis of spherical geometry approximation ($f/f_o = 1$) and $S^o_{20,w}$ for monomer of 13.1 S. Values in bold have been used to draw theoretical curves through experimental data points in Figure 2 and for determination of weight distribution of species in Figure 4.

monomer ⇌ tetramer or multistate models involving higher aggregates. Although the following analysis focuses on data based on a spherical geometry approximation (Table 2), generally the same conclusion can be derived from data based on other geometry assumption (Table 3). After a quick survey of the results shown in Table 2, it is clear that the mode of self-association of core protein must involve a mechanism that does not include cooperative binding of oligomers to form higher aggregates, a finding supported by the observation of no bimodality in sedimentation patterns. However, it is interesting to note that curve-fitting of the weight-average sedimentation coefficient data in 0.01 M NaCl buffer indicated a possibility of monomer ⇌ trimer stoichiometry of aggregation. The extreme nonideal behavior exhibited by the core protein in this buffer with low salt concentration may be the cause for not observing bimodal patterns even though a monomer ⇌ trimer stoichiometry was indicated in data fitting. Other modes of aggregation that might yield bimodal patterns under the same conditions were discounted on the basis that the associated SS values are at least one order of magnitude greater than that for monomer ⇌ trimer equilibrium. A closer examination of the results of fitting of data at higher NaCl concentrations indicates that this mode of monomer ⇌ trimer aggregation cannot be the correct mode to describe the associating behavior of core protein in all NaCl concentrations as the SS values are significantly higher in these experimental conditions. Since the same conclusion can be derived for RNA polymerase oligomers of different geometry, the assumption involved in the geometry of RNA polymerase *does not* affect the basic conclusion in excluding a cooperative model for further consideration.

The only models that adequately describe the mode of self-association of *E. coli* RNA polymerase core protein are sequential modes of protein aggregation for which the Gilbert (1955) theory does not predict bimodality, as indicated by the consistently low SS values deserved for the model. SS values for sequential self-association models invoking ag-

Table 3: Summary of Fitted Equilibrium Intrinsic Association Constants for Self-Association of *E. coli* RNA Polymerase Core Protein as a Function of NaCl Concentration[a]

	K_2 (mL/mg)		K_3 (mL/mg)^2		K_4 (mL/mg)^3			SS	
[NaCl] (M)	oblate	prolate	oblate	prolate	oblate	prolate	g	oblate	prolate
0.01	0.51	*0.13*	3.95×10^4	*1.06×10^5*			0.13	111	*124*
	0.58	*1.96*	392	*268*	6767	*8224*	0.13	8.62	*8.60*
	60	*30.4*			6.00×10^4	*3.10×10^4*	0.13	11.1	*9.64*
0.05	8.65	*1.40*	1922	*1650*			0	3.51	*3.49*
	50.5	*7.20*	3492	*1787*	8325	*1243*	0	3.20	*3.39*
	2235	*1443*			8.54×10^6	*4.36×10^6*	0	7.23	*7.15*
0.08	12.7	*12.5*	62.4	*65.9*			0	5.18	*5.19*
	24.0	*20.9*	0.41	*21.9*	343	*255*	0	3.81	*3.90*
	24.0	*24.2*			344	*384*	0	3.84	*3.82*
0.15	0.59	*0.60*	0.37	*0.33*			0	12.2	*12.4*
	0.62	*0.65*	0.32	*0.25*	2.64×10^{-3}	*0.08*	0	12.1	*12.2*
	0.75	*0.77*			0.28	*0.30*	0	12.6	*12.5*
0.18	0.001	*7.12×10^{-4}*	0.11	*0.12*			0	0.62	*0.64*
	0.03	*2.56×10^{-8}*	0.09	*1.10*	0.01	*9.87×10^{-3}*	0	0.80	*0.65*
	0.08	*8.53×10^{-2}*			0.05	*5.15×10^{-2}*	0	0.91	*0.89*

[a] Values for thermodynamic parameters governing self-association have been obtained using eq 2 where sedimentation coefficients of oligomers have been calculated from consideration of higher oligomers as either oblate or prolate ellipsoids of revolution having appropriate axial ratios. Under colums oblate and prolate are values of K_i obtained for oblate and prolate ellipsoids of revolution, respectively.

gregation beyond trimer are essentially unchanged. Therefore, on the basis of SS values alone it is not possible to rule out models of protein self-association beyond trimer, but they may reasonably be excluded on the grounds that the equilibrium intrinsic association constants for self-association to higher aggregates (i.e., K_4, K_5, etc.) are considerably smaller than K_3. Hence, sequential self-association of core protein monomers to form trimer was chosen as the simplest model to describe the aggregation phenomenon on the basis of rules established for similar investigations of phosphofructokinase (Luther et al., 1986; Cai et al., 1990) and listed in Materials and Methods.

The excellent fit of theoretical curves drawn through data points in Figure 2 visually indicates that the association constants and stoichiometry of aggregation characterizing the sequential model of association adequately describe the behavior of core RNA polymerase. The values for hydrodynamic nonideality coefficient (g) quoted in Table 2 are those that yielded lowest SS value in conjunction with floated values for equilibrium intrinsic association constants. The fitted value of 0.13 mL/mg in 0.01 M NaCl buffer is in good agreement with that of 0.12 mL/mg determined experimentally. At other salt concentrations tested in this manner, the value of g yielding the lowest SS is zero; SS increases in hyperbolic manner when fits are repeated with g constrained to be greater than zero and the K_i's are floated (data not shown).

Theoretically determined parameters that describe core protein self-association have not been presented for experimental data obtained in 0.20 M NaCl buffer. Various combinations of small values for equilibrium association constants provided equally good fits to experimental data, thereby not allowing discrimination of thermodynamic parameters that describe core protein self-association at this particular salt concentration. Thus, the curve drawn through this particular set of experimental data points merely indicates the trend of data.

At NaCl concentrations higher than 0.01 M, models describing sequential self-association to trimer or tetramer can fit the experimental data well. An alternative model involving successive dimerizations (monomer $\rightleftharpoons$ dimer $\rightleftharpoons$ tetramer) also provides adequate description of core protein self-association at most NaCl concentrations. It is not surprising that the stoichiometry is extended to tetramer for the protein with nonspherical geometry (Table 3). This is a natural consequence of the fact that asymmetric macromolecules are characterized by small values for $S^{\circ}_{20,w}$ (Table 1); thus, the same numerical value of $\bar{S}_{20,w}$ would imply the presence of species of larger stoichiometry. Although a consideration of RNA polymerase core protein aggregates as either spheres or ellipsoids represent the extreme limits, the important feature to arise from these studies is that a sequential model of self-association provides the best description for this system and eliminates further serious consideration of cooperative model.

Having determined the thermodynamic parameters that govern the self-association of core RNA polymerase, it is useful to know the distribution of all oligomeric species present in solution as a function of total protein concentration. Species distributions have been determined for two sequential self-association schemes terminating at trimer and tetramer, respectively, where oligomers obey the spherical geometry approximation. Extreme hydrodynamic nonideality in 0.01 M NaCl buffer effectively precludes meaningful analysis. Both sequential self-association schemes yield essentially identical oligomer distributions, there being maximally less than 2% tetramer at the highest protein concentration used in these experiments and at all salt concentrations. Therefore, it is appropriate to discount further serious consideration of self-association of RNA polymerase core protein beyond trimer. Weight-percent distributions of oligomers in TED + 0.15 M NaCl are presented in Figure 4.

Simulation of Velocity Sedimentation Boundary and Derivative Profiles. A powerful tool to define the mode of macromolecular association is to compare and contrast the simulated and experimental sedimentation profiles. Bimodality in the derivative profiles of the sedimentation boundary is predicted for cooperative associating systems when $n \geq 3$ (Gilbert, 1955, 1959). No evidence of bimodality was observed in the present sedimentation velocity experiments, a finding in accordance with the self-association scheme determined from curve-fitting. Therefore, in order to further assess the validity of this proposed sequential model of core

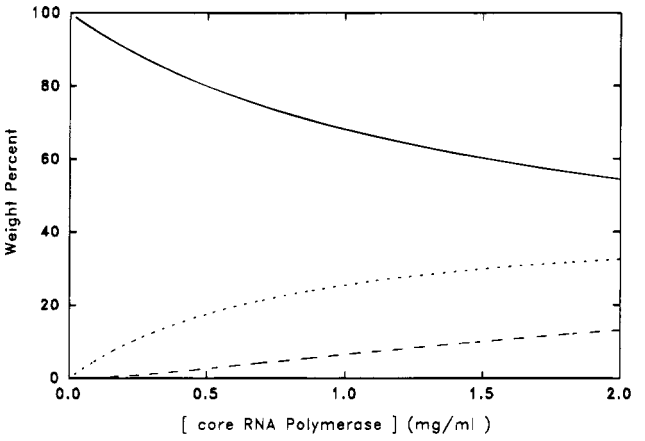

FIGURE 4: Weight distribution of oligomeric species for *E. coli* RNA polymerase core protein undergoing sequential self-association of monomer terminating at trimer. Curves are theoretical distributions of monomer (solid line), dimer (short-dash line) and trimer (long-dash line) in TED + 0.15 M NaCl calculated from nonlinear computer curve-fitting routine (see text).

protein self-association, an extensive study of simulated velocity sedimentation boundary and derivative profiles was undertaken. Thermodynamic parameters obtained for the self-association scheme determined for globular (spherical) and ellipsoid aggregates have been used to simulate profiles for system exhibiting monomer ⇌ dimer ⇌ trimer equilibrium.

Simulations of velocity sedimentation boundary and derivative profiles were performed on a IBM PS/2 personal computer using minor modifications of the routine developed by Cox and Dale (1981). Diffusion coefficients for *n*-mers were determined by use of the Svedberg equation and sedimentation coefficients (Table 1) for appropriate aggregation scheme. Values of K_i used in simulations of sedimentation profiles for sequential self-association scheme for core protein are those listed in Tables 2 and 3. Simulated profiles for both self-association schemes proposed for *E. coli* RNA polymerase core protein are presented in Figure 5. Simulations of velocity sedimentation derivative profiles for the sequential self-association model (Figure 5b,d) do not exhibit bimodal patterns, a finding in agreement with classical Gilbert theory for associating systems; similar patterns are observed for both cases of geometric extremes. These simulated results based on the sequential model are in good agreement with the experimental data as shown in Figure 3.

The theory for sedimentation behavior of an associating system predicts the observation of bimodality in the sedimentation profiles of a cooperative model proposed by Shaner et al. (1982), but such an observation was not reported. Hence, in an effort to identify the cause of the difference in conclusions between the study by Shaner et al. and this report, simulations of core protein undergoing cooperative self-association have been performed using values of K_4 deduced from Figure 8 of Shaner et al. (1982), where oligomers have been assumed to obey the spherical geometry approximation. Similar simulations have been performed for oligomers considered as ellipsoids of revolution. Simulations were performed for 30 min velocity sedimentation at 32 000 rpm using the average core protein concentration (0.29 mg/mL) used in previous study (Shaner et al., 1982) or at 52 000 rpm and the same indicated core protein concentration in order to mimic the experimental conditions of this study and to allow direct comparison of profiles for differing modes of self-association.

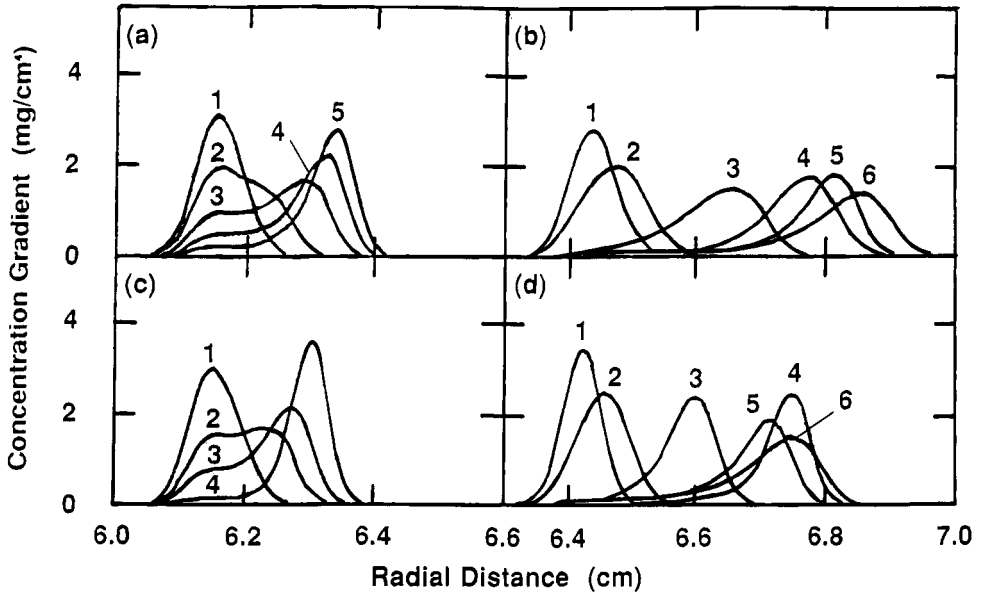

FIGURE 5: Simulated velocity sedimentation protein concentration gradient profiles for RNA polymerase core protein undergoing different self-association equilibria. Profiles were obtained using distorted-grid simulation routine (Cox & Dale, 1981). Values of sedimentation coefficients, diffusion coefficients, and appropriate equilibrium intrinsic association constants used in these simulations are described in text. Panels a and c are simulations for two-state model of core protein self-association where oligomers are considered as either spheres or prolate ellipsoids, respectively, at NaCl concentrations of (1) 0.228 M, (2) 0.190 M, (3) 0.167 M, (4) 0.121 M, and (5) 0.079 M. Protein concentration = 0.29 mg/mL, rotor speed = 32 000 rpm, duration = 30 min, and g = 0.007 mL/mg for all simulated profiles. Panels b and d are simulations for sequential model of core protein self-association, oligomers considered as spheres and prolate ellipsoids, respectively. NaCl concentrations are (1) 0.18 M, (2) 0.15 M, (2)0.15 M, (3) 0.08 M, (4) 0.05 M, and (5) and (6) 0.01 M. Protein concentration = 0.29 mg/mL, rotor speed = 52 000 rpm, duration = 30 min, and g = 0.007 mL/mg at all salt concentrations; profiles were also abtained for self-association at 0.01 M NaCl(5) where g = 0.13 mL/mg in accordance with best-fit value of hydrodynamic nonideality coefficient obtained from nonlinear regression analysis through experimental data.

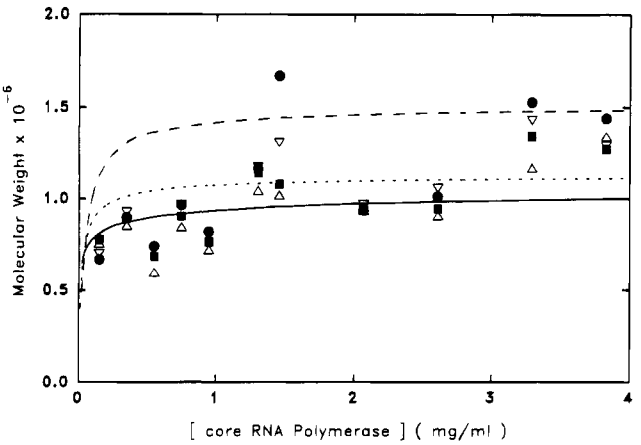

FIGURE 6: Protein concentration dependence of weight-average molecular weight of *E. coli* RNA polymerase core protein. Results were obtained, as described in the text, from small-angle light scattering experiments performed using core protein in TED buffer (pH 7.8) containing 0.05 M NaCl at 20 °C. Scattering angles used were (●) 2−3°, (▽) 3−4°, (■) 4.5−5.5°, and (△) 6−7°. Curves drawn through experimental data points represent theoretical dependence of weight-average molecular weight as function of core protein concentration: (- - -) protein exhibiting cooperative monomer−tetramer mode of self-association, and sequential self-association of monomer to trimer where oligomers are considered as sphere (—) and prolate ellipsoids (• • •), respectively.

Profiles obtained for two-state monomer ⇌ tetramer stoichiometry of core protein self-association are presented in Figure 5 panels a and c for spherical and prolate ellipsoid oligomers, respectively, as a function of NaCl concentration. Bimodality is clearly apparent in these simulated protein concentration derivative profiles in agreement with predictions based on Gilbert theory (1955, 1959, 1963) for a self-associating protein where $n \geq 3$. Under the specific set of experimental conditions, only a single peak will be observed at high salt concentration; as salt concentration is decreased, a second faster-moving peak becomes apparent with concomitant decrease in the size of the slower-moving peak.

In most of these simulated profiles a value of 0.007 mL/mg was used for hydrodynamic nonideality coefficient by assuming that the protein is globular. For low salt condition at 0.01 M NaCl, simulations have also been performed using the fitted hydrodynamic nonideality coefficient of 0.13 mL/mg in order to illustrate the severe effect of solution nonideality prevalent at this experimental condition. Bimodality is clearly evident for core protein exhibiting cooperative self-association at the low concentration (0.29 mg/mL) used in previous study (Shaner et al., 1982) even in the presence of such nonideal solution environment. Thus, nonideality is unlikely to be the cause for the failure to observe bimodality by Shaner et al.

Light Scattering Studies of Core Protein Self-Association. In order to acquire additional information on the sequential model of core protein self-association, studies by small-angle light scattering of core protein solutions were conducted at fixed NaCl concentration (0.05 M).

It is evident from the results presented in Figure 6 the efforts to remove dust from protein solution has not been completely successful. Although it was not possible to obtain accurate estimates of weight-average molecular weights of protein solutions from resultant Zimm plots (data not shown), the measured values of M_w do represent an upper bound to the true values and can be examined for consistency with the models used to fit the sedimentation data. Theoretical protein concentration dependence of $\overline{M}_w$ was determined by use of the data from calculated oligomeric species distributions (eq 2) for the cooperative and sequential models of core protein self-association. Values for K_2 and K_3 for sequential self-association are those presented in Table 2 for spherical oligomers and Table 3 for prolate ellipsoids of revolution: the appropriate value of K_4 has been deduced from Figure 8 of Shaner et al. (1982) for cooperative formation of tetrameric oligomer. The curves drawn through Figure 6 represent theoretically determined weight-average molecular weights ($\overline{M}_w$) for sequential monomer ⇌ dimer ⇌ trimer self-association (solid line, spherical oligomer geometry; short-dash line, prolate ellipsoid oligomer geometry) and cooperative monomer−tetramer aggregation (long-dash line, spherical oligomer geometry). Owing to the extent of noise from "dust" in core protein solutions, one cannot definitively discriminate between theoretical curves determined for spherical and ellipsoid oligomers; however, the bad fit observed for cooperative self-association scheme, where oligomers have been considered as spheres only, further supports the conclusion that the cooperative mode of association does not adequately describe data from this study.

DISCUSSION

The self-association of *E. coli* core RNA polymerase was studied by a combination of sedimentation velocity experiments and computer simulation. The only self-consistent model that can best describe the data under all experimental conditions employed in this study is a sequential model. This conclusion is consistent with the results of small-angle X-ray study by Heumann et al. (1982). The cooperative model proposed by Shaner et al. (1982) is not compatible with the results of this study. One of the evidences that is inconsistent with the cooperative model is the absence of bimodality in the sedimentation profiles, which contain a wealth of information. While bimodality may be clearly evident in derivative profiles, which correspond to Schlieren patterns, evidence of bimodality cannot always be clearly observed at low protein concentrations from a casual survey of the moving-boundary profiles which are recorded by UV scanner attached to Model E analytical ultracentrifuge. Simulated moving-boundary and derivative profiles are employed to illustrate this important point, as shown in Figure 7. The experimental conditions of Shaner et al. (1982) were chosen for this simulation. It is evident that bimodality in the derivative profiles is observable even for a short sedimentation run of 30 min. The reaction boundary corresponding to the slow-moving peak exhibits no special feature except an elevation from the baseline. The accuracy to define the value of $\bar{s}$ depends on the ability to precisely determine the end point of the reaction boundary. At low protein concentrations, the signal to noise ratio will significantly increase rendering the precise location of the end points of the reaction boundary even more difficult. This difficulty is further aggravated in defining the boundary with longer durations of sedimentation due to the additional spreading of the reaction boundary. An error in defining the end point toward the meniscus will lead to an erroneously high $\bar{s}$ value. The difficulty in defining the end-points may contribute towards the significantly higher $\bar{s}$ values reported by Shaner et al. For example, in Figure 7C, the value of $S_{20,w}$ for the fast-

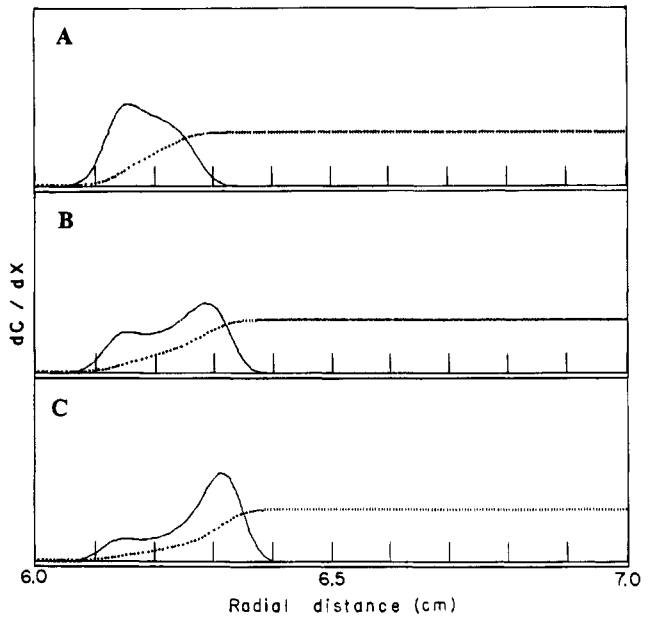

FIGURE 7: Simulated sedimentation velocity profiles of RNA polymerase core protein at 0.29 mg/mL, 32 000 rpm, 1800 s of sedimentation time, $S^{\circ}_{20,w}$ and $D^{\circ}_{20,w}$ for monomer and tetramer are 11.9S/2.76 × 10^{-7} cm^2/S and 28.1S/1.63 × 10^{-7} cm^2/S, respectively. The [Cl^-] in M and K_4 in M^{-3} are as follows: (A) 0.19, 2.51 × 10^{17}; (B) 0.167, 2.51 × 10^{18}; and (C) 0.143, 1.58 × 10^{19}. In each frame, the derivative curve is superimposed on the reaction boundary.

moving peak is 25 S while the value of $\bar{S}_{20,w}$ is 19.4 S. Under the same experimental condition, the value of $\bar{S}_{20,w}$ reported by Shaner et al. is approximately 24 S. Thus, it is conceivable that the difference between the conclusions of studies by Shaner et al. and this laboratory is not in the data but in the procedure of data analysis. It is imperative that in any study of macromolecular assembly by sedimentation velocity a careful analysis of the derivative profiles of the reaction boundary be conducted. The shape of these profiles contains a wealth of information pertaining to the mode of association.

It should also be noted that Shaner et al. included at least 3% glycerol in their experiments, a situation which could contribute significant thermodynamic nonideality from inclusion of inert space-filling solute in reaction mixture. Such effects of inert solute would be expected to enhance an existing equilibrium to favor the formation of large aggregates (Lee & Timasheff, 1977; Harris & Winzor, 1985; Shearwin & Winzor, 1988). Thus, in the present case, the amount of tetramer would be increased at the expense of monomer, thereby making identification of slower peak difficult, if not impossible.

In accordance with previous findings, Shaner et al. (1982) showed that the self-association of core RNA polymerase is an anion-linked phenomenon. Hence, the chloride dependence of equilibrium intrinsic association constants describing aggregate formation is presented in Figure 8. The equilibrium intrinsic association constants in this figure are presented having units of M^{n-1}. They are related to values reported in Table 2 by the relationship

$$k_n = K_n M_1^{n-1}/n \qquad (4)$$

where M_1 is the molecular weight of monomeric RNA polymerase core protein (380 000). This plot clearly shows

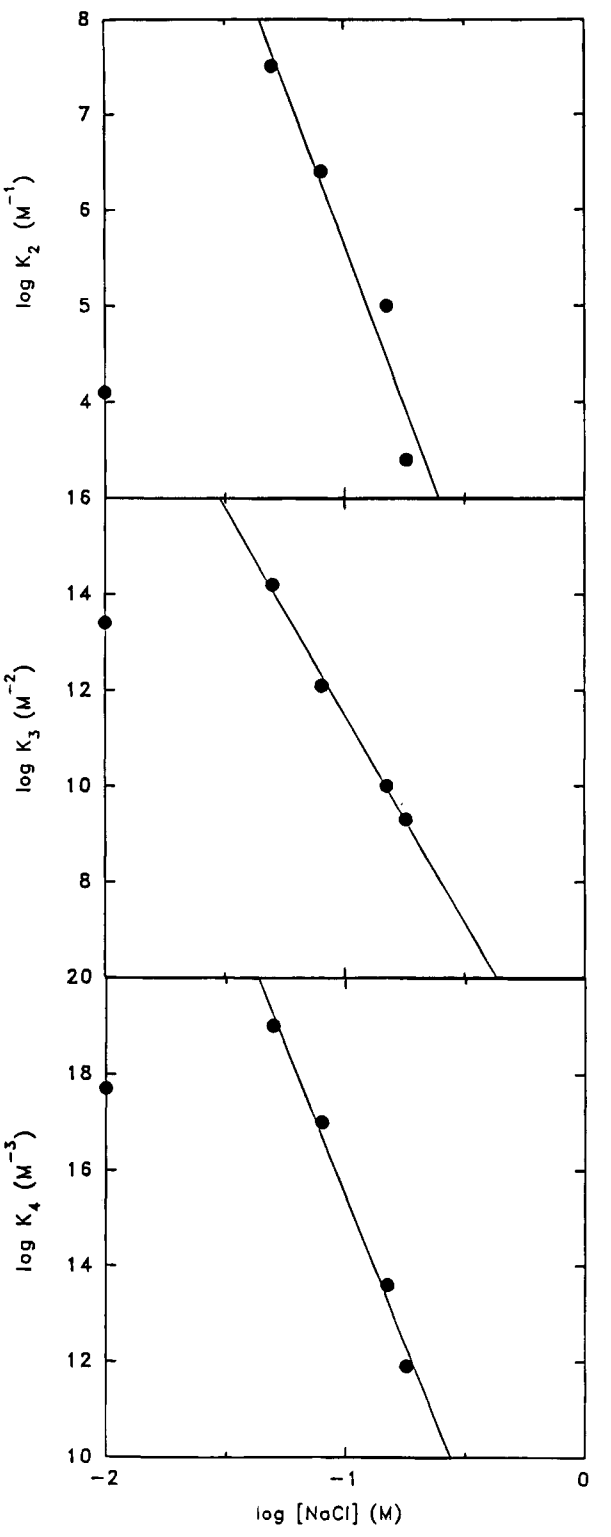

FIGURE 8: Dependence of fitted equilibrium constants for formation of RNA polymerase core protein aggregates upon NaCl concentration. Adair constants having appropriate molar units have been calculated from data summarized in Table 2 and eq 4 where higher aggregates have been considered to obey spherical geometry approximation. The line drawn through the data is linear least-squares regression line excluding data obtained in TED buffer containing 0.01 M NaCl.

a typical Wyman (1964) dependence of association constants for sequential dimer and trimer formation (k_2 and k_3) upon NaCl concentration. Apparent equilibrium intrinsic association constants for core protein aggregation in 0.01 M NaCl buffer are all depressed and do not obey linear linked-

Table 4: Intrinsic Association Constants Defining Binding of Successive Monomeric Subunits in RNA Polymerase Core Protein Aggregation Phenomenon[a]

[NaCl] (M)	scheme	k_2 (M^{-1})	k_3 (M^{-1})	k_4 (M^{-1})
0.01	1−2−3	3.61×10^4	6.59×10^8	
	1−2−3−4	3.99×10^4	6.35×10^8	2.27×10^4
0.05	1−2−3	3.21×10^7	5.25×10^6	
	1−2−3−4	3.65×10^7	5.30×10^6	5.53×10^4
0.08	1−2−3	2.45×10^6	4.62×10^5	
	1−2−3−4	2.51×10^6	4.08×10^5	9.97×10^4
0.15	1−2−3	1.05×10^5	9.63×10^4	
	1−2−3−4	1.08×10^5	8.91×10^4	3.58×10^3
0.18	1−2−3	1.90×10^3	2.03×10^3	
	1−2−3−4	1.90×10^3	2.03×10^3	2.14×10^5

[a] Calculated from Adair association constants presented in Table 2 and converted to molar units using eq 4 for system where aggregate species have been considered to obey spherical geometry approximation: microconstants for core protein self-association are defined where $K_2 = k_2$, $K_3 = k_2k_3$, and $K_4 = k_2k_3k_4$.

function relationship. This represents another manifestation of hydrodynamic nonideality arising from primary charge effect as evidence (see Figure 2) from protein concentration dependence of the weight-average sedimentation coefficient at this salt concentration. Consequently, lines drawn through data points represent linear least-squares regression excluding data at low NaCl concentration. From slopes of these regression lines, each core protein monomer releases 3.6 ± 0.70, 2.8 ± 0.23, and 3.1 ± 0.24 chloride ions per contact upon association to dimer, trimer and tetramer aggregate species, respectively. Thus, it can be reasonably concluded that each core protein monomer releases three chloride counterions per contact upon self-association to higher oligomeric species.

Equilibrium constants determined for core protein self-association are Adair constants for equilibrium between monomer and *i*-mer species which can be related to intrinsic microconstants for binding of successive core protein monomers (k_i, having M^{-1} units), where

$$K_2 = k_2$$

$$K_3 = k_2k_3$$

$$K_4 = k_2k_3k_4 \quad (5)$$

Dissected intrinsic microconstants are summarized in Table 4. It is apparent that binding affinity of second and third monomers are approximately equivalent, there being slight negative cooperativity of trimer formation at salt concentrations greater that 0.05 M. Binding of further monomer to form higher aggregate species involves higher degree of negative cooperativity of binding. Therefore, it can be reasonably concluded that although self-association of RNA polymerase core protein apparently involves sequential addition of monomer in formation of higher oligomers the actual mechanism does not involve classical isodesmic self-association (van Holde, 1975) wherein standard enthalpy change is identical for each successive monomer addition and standard entropy change is similarly identical (Garland & Christian, 1975; Adams et al., 1978). However, in a purely qualitative sense, the observed decrease in theoretically determined successive equilibrium microconstants (k_i) is suggestive of the attenuated equilibrium constant (AK) model variant (Garland & Christian, 1975) of the more tradition sequential equilibrium constant (SEK) model (Garland & Christian, 1975; Adams et al., 1978) which has been successfully applied in analysis of indefinitely self-associating systems (Beckerdite et al., 1980). The AK model proposes that there should be varying entropy changes such that equilibrium constants (k_i) are systematically attenuated for each successive step, thus $k_3 = k_2/2$ and $k_4 = k_3/3$, etc. The model-fitting attempts in this study have included efforts to constrain values of K_i in order to accommodate the sequential model for core protein self-association with both SEK and AK models of isodesmic self-association; however, to date, these attempts have only resulted in a failure to converge on meaningful values.

On the basis of the results of this study it is clear that core protein self-association phenomenon exists at physiologically relevant conditions of pH and salt concentration with all oligomers being present in solution. A significant proportion of intracellular RNA polymerase exists as core protein *in vivo* since purified protein displays variable extent of saturation with σ factor, ranging from 40 to 80% saturation (Berg et al., 1971; Lowe et al., 1979). The extent of saturation of core protein with σ factor *in vivo* has been estimated to be as low as 40−30% (Burgess, 1976). Estimates based on typical purification yields of 100−400 mg of protein per kg of wet cells (Burgess, 1971) indicate that RNA polymerase core protein exists as an equilibrium mixture of oligomers comprising 87−96% monomer, 3.7−11% dimer, and 0.3−2% trimer *in vivo*. In fact, the situation pertaining *in vivo* is likely to be even more complex once account is taken of thermodynamic nonideality effects arising from presence of inert solutes which crowd the intracellular milieu. This "molecular crowding" effect would enhance protein interaction equilibria (Harris & Winzor, 1985; Shearwin & Winzor, 1988; Lee & Timasheff, 1977; Jarvis et al., 1990), a point which has not been addressed in the investigation. The present *in vitro* study was conducted in the absence of cellular milieu which will render the system thermodynamically nonideal. Such nonideality may be mimicked by macromolecular crowding. In view of the recent recognition of the potential importance of "macromolecular crowding" in macromolecular assembly (Jarvis et al., 1990; Zimmerman, 1994), it is important that the self-associating properties of the enzyme, which plays such a central role in transcription, be systematically characterized.

ACKNOWLEDGMENT

We thank Dr. Xiaodong Cheng for his critical input on this work and Dr. Rajendran Surendran for the presentation of data in Figure 3.

REFERENCES

Adams, E. T., Jr., Tang, L. H., Sarquis, J. L., Barlow, G. H., & Norman, W. M. (1978) in *Physical Aspects of Protein Interactions* (Catsimpoolas, N., Ed.) pp 1−55, Elsevier North Holland, Inc., New York.

Arisaka, F., & Van Holde, K. E. (1979) *J. Mol. Biol. 134*, 41−73.

Beckerdite, J. M., Wan, C. C., & Adams, E. T., Jr. (1980) *Biophys. Chem. 12*, 199−214.

Berg, D., & Chamberlin, M. (1970) *Biochemistry 9*, 5055−5064.

Berg, D., Barrett, K., & Chamberlin, M. (1971) *Methods Enzymol. 21D*, 506−519.

Blazy, B., Takahashi, M., & Baudras, A. (1980) *Mol. Biol. Rep. 6*, 39−43.

Burgess, R. R. (1969a) *J. Biol. Chem. 244*, 6160−6167.
Burgess, R. R. (1969b) *J. Biol. Chem. 244*, 6168−6176.
Burgess, R. R. (1971) *Annu. Rev. Biochem. 40*, 711−740.
Burgess, R. R. (1976) in *RNA Polymerase* (Losick, R., & Chamberlin, M. J., Eds.) pp 69−100, Cold Spring Harbor Laboratory, Cold Spring Harbor, NY.
Burgess, R. R., & Jendrisak, J. J. (1975) *Biochemistry 14*, 4634−4638.
Burgess, R. R., Travers, A. A., Dunn, J. J., & Bautz, E. K. F. (1969) *Nature 221*, 43−46.
Cai, G.-Z., Lee, L. L.-Y., Luther, M. A., & Lee, J. C. (1990) *Biophys. Chem. 37*, 97−106.
Callaci, T. P., Cai, G.-Z., Lee, J. C., Daly, T. J., & Wu, C.-W. (1990) *Biochemistry 29*, 4653−4659.
Cann, J. R. (1970) *Interacting Macromolecules: Theory and Practice of Their Electrophoresis, Ultracentrifugation and Chromatography*, pp 249, Academic Press, New York.
Chamberlin, M. J. (1976) in *RNA Polymerase* (Losick, R., & Chamberlin, M. J., Eds.) pp 159−191, Cold Spring Harbor Laboratory, Cold Spring Harbor, NY.
Chamberlin, M., Nierman, W., Wiggs, J., & Neff, N. (1979) *J. Biol. Chem. 254*, 10061−10072.
Cox, D. J., & Dale, R. S. (1981) in *Protein−Protein Interactions* (Frieden, C., & Nichol, L. W., Eds.) pp 173−211, Wiley and Sons, New York.
Garland, F., & Christian, S. D. (1975) *J. Phys. Chem. 79*, 1247−1252.
Gilbert, G. A. (1955) *Discuss. Faraday Soc. 2*, 68−71.
Gilbert, G. A. (1959) *Proc. R. Soc. London A 250*, 377−388.
Gilbert, G. A. (1963) *Proc. R. Soc. London A 276*, 354−366.
Harris, S. J., & Winsor, D. J. (1985) *Arch. Biochem. Biophys. 342*, 598−604.
Hesterberg, L. K., & Lee, J. C. (1981) *Biochemistry 20*, 2974−2980.
Hesterberg, L. K., & Lee, J. C. (1982) *Biochemistry 21*, 216−222.
Heumann, H., Meisenberger, O., & Pilz, I. (1982) *FEBS Lett. 138*, 273−276.
Heyduk, T., Lee, J. C., Ebright, Y. W., Blatter, E. E., Zhou, Y. H., & Ebright, R. H. (1993) *Nature 364*, 548−549.
Jarvis, T. C., Ring, D. M., Daube, S. S., & von Hippel, P. H. (1990) *J. Biol. Chem. 265*, 15160−15167.
Lee, J. C., & Timasheff, S. N. (1977) *Biochemistry 16*, 1754−1764.
Lowe, P. A., Hager, D. A., & Burgess, R. R. (1979) *Biochemistry 18*, 1344−1352.
Luther, M. A., Cai, G.-Z., & Lee, J. C. (1986) *Biochemistry 25*, 7931−7937.
Malan, T. P., Kolb, A., Buc, H., & McClure, W. R. (1984) *J. Mol. Biol. 180*, 881−909.
Marquardt, D. W. (1963) *J. Soc. Ind. Appl. Math. 11*, 431−440.
Nichol, L. W., Bethune, J. L., Kegeles, G., & Hess, E. L. (1964) *The Proteins (2nd. ed.) 2*, 305−403.
Nissley, P., Anderson, W. B., Gallo, M., Perlman, R. L., & Pastan, I. (1972) *J. Biol. Chem. 247*, 4264−4269.
Pilz, I., Kratky, O., & Rabussay, D. (1972) *Eur. J. Biochem. 28*, 205−220.
Pinkney, M., & Hoggett, J. G. (1988) *Biochem. J. 250*, 897−902.
Richardson, J. P. (1966) *Proc. Natl. Acad. Sci. U.S.A. 55*, 1616−1623.
Schachman, H. K. (1959) *Ultracentrifugation in Biochemistry*, pp 272, Academic Press, New York.
Shaner, S. L., Platt, D. M., Wensley, C. G., Yu, H., Burgess, R. R., & Record, M. T., Jr. (1982) *Biochemistry 21*, 5539−5551.
Shearwin, K. E., & Winsor, D. J. (1988) *Biophys. Chem. 31*, 287−294.
Spassky, A., Busby, S., & Buc, H. (1984) *EMBO J. 3*, 43−50.
Stevens, A., Emery, A. J., Jr.,, & Sternberger, N. (1966) *Biochem. Biophys. Res. Commun. 24*, 929−936.
Teller, D. C. (1973) *Methods Enzymol. 27*, 346−441.
Travers, A. A., & Burgess, R. R. (1969) *Nature 222*, 537−540.
Travers, A. A., Lamond, A. J., & Mace, H. A. F. (1982) *Nucleic Acids Res. 10*, 5043−5057.
van Holde, K. E. (1975) *The Proteins (3rd. ed.) 1*, 225−291.
Williams, R. C. 1986) *Methods Enzymol. 130*, 35−47.
Wu, F. Y.-H., Nath, K., & Wu, C.-W. (1974) *Biochemistry 13*, 2567−2572.
Wu, C.-W., Yarbrough, L. R., Hillel, Z., & Wu, F. Y.-H. (1975) *Proc. Natl. Acad. Sci. U.S.A. 72*, 3019−3023.
Wyman, J. (1964) *Adv. Protein Chem. 19*, 223−286.
Zimmerman, S. B. (1993) *Biochim. Biophys. Acta 1216*, 175−185.

BI950415A